ISSN 1814-4225 (print)
ISSN 2663-2012 (online)

UDC 621.3-042.3:535-3 doi: 10.32620/reks.2026.1.13

Viktoriia ABRAMOVA[1,2], Sergiy ABRAMOV[1,2], Linas MINKEVIČIUS[2], Ignas GRIGELIONIS[2]

[1] ***National Aerospace University "Kharkiv Aviation Institute", Kharkiv, Ukraine***
[2] ***Center for Physical Sciences and Technology, Vilnius, Lithuania***

ENHANCING TERAHERTZ IMAGES CORRUPTED BY COMPACT IMPULSE NOISE: FEASIBILITY AND PRACTICAL RECOMMENDATIONS

*The **subject matter** of this article is the process of enhancing low-quality terahertz images through digital image processing. This study **aims** to investigate whether the visual quality of terahertz images corrupted by compact impulse noise can be improved while preserving their information value. The **tasks** to be solved are as follows: 1) to analyze impulse noise in real-life terahertz images obtained by raster scanning systems and to evaluate the typical range of its probabilities and localization features; 2) to create an adequate model for compact impulse noise generation; 3) to establish a relation between the probability of impulse noise, image spatial resolution, filtering settings, and the quality of the output images, and give the corresponding recommendations; and 4) to verify the obtained results on real-life terahertz data. The **methods** used are: mathematical modelling, numerical simulation, and statistical analysis. The following **results** were obtained. 1) The shape and localization characteristics of compact impulse noise in terahertz images acquired using a single-detector direct imaging setup were studied, and an appropriate generative statistical model was implemented. 2) The possibility of suppressing stripe-shaped compact impulse noise using a classical median filter and its modification with spatial adaptation was investigated through numerical simulations on a set of test images. 3) It was shown that for images no less than 100×100 pixels large and impulse noise probability up to 0.5, filtering with vertically oriented rectangular windows (9×1 to 15×1 pixels) allows quality improvement up to 45 dB according to PSNR and PSNRHVSM metrics, providing effective noise suppression while preserving object details. 4) The formulated recommendations' adequacy was verified on real-life terahertz data, and the proposed approach's workability in the presence of other distortions was confirmed. **Conclusions.** The scientific novelty of the obtained results is in the confirmation of the possibility of reliable restoration of terahertz images severely distorted by compact impulse noise without their re-acquisition along with providing practical recommendations for filtering settings and the requirements to the input terahertz data.*

Keywords: *image processing; quality enhancement; terahertz images; compact impulse noise; raster scanning systems.*

1. Introduction

1.1. Motivation

Owing to the lack of efficient emitters and detectors, the frequency range between 0.1 and 10 terahertz (THz) is usually referred to as "terahertz gap". However, with the development of technology [1, 2], this gap is being gradually closed from both sides, allowing more novel applications relying on the unique properties of THz waves [3, 4]. The non-ionizing nature of THz radiation, millimeter to sub-millimeter wavelengths, providing sufficient spatial resolution and high penetration through non-conducting materials, open promising perspectives in non-destructive testing [5, 6], security screening [7, 8], biomedical imaging [9, 10], art inspection [11, 12], and cultural heritage conservation [13, 14].

Nevertheless, despite the progress in imaging equipment and methods [1, 2], the obtained THz images still often have low visual quality, suffering from intense noise [15, 16], blur [17, 18], and interference patterns in amplitude [19, 20]. Therefore, their enhancement before applying any information extraction procedures (e.g., object identification or edge detection) or visual inspection by an expert is highly desirable.

In recent years, the interest in processing THz images has grown rapidly [1, 21]; however, its progress has encountered many challenges and limitations [2, 3]. The main problem is that the quality of THz images is affected by the shooting conditions, alignment of setup elements, material of the object under study, and equipment parameters [1, 2]; thus, it can greatly differ even for the same object and setup [15].

Another common issue in THz imaging is the low image acquisition speed [2, 22]. Because of the use of single-pixel sensors, raster scanning is required to obtain a full image of an object, which ranges the image acquisition time from tens of minutes to tens of hours depending on the

desired spatial resolution and the size of a specimen. Besides, the presence of moving elements in an imaging setup creates risks for additional types of distortion [23, 24], such as motion blur [17, 20] or impulse noise [25, 26]. The latter might have quite high probability and take on a compact form [24, 27], thus making it a relevant quality degrading factor that is also more difficult to remove.

Owing to the abovementioned peculiarities, the set of distortions present in THz images in each particular case, as well as their severity, become nearly unpredictable, making the development of quality enhancement methods possessing any versatility virtually impossible. Currently, all such methods are developed for each dataset, whereas these datasets are often quite limited [15, 28]. Adequate models describing possible distortions are also lacking [17, 29].

Nevertheless, although highly specialized, each solved quality analysis or enhancement task adds to the general knowledge base, expanding the understanding of distortion mechanisms in THz images and their variety. This paves the way for developing comprehensive distortion models that will allow the creation of more universal solutions for their elimination. Furthermore, the analysis of quality problems in real-life THz data helps to understand how the equipment and image acquisition process can be improved to decrease the level of distortions and/or ease the future process of their elimination.

This article addresses a specific challenge in improving the quality of THz images, namely, the removal of compact impulse noise. The primary focus will be on developing practical recommendations for both image acquisition and filtering processes that will allow to effectively eliminate such noise while introducing minimal distortion into the image information content.

1.2. State of the art

Considerable advances have been made in the field of THz imaging equipment over the past three decades [1, 2]. In particular, there has been an active search for alternatives to raster scanning [1, 30], leading to many THz imaging systems that use sensor arrays or their matrices [31, 32]. However, such systems are significantly more expensive and often provide lower signal-to-noise ratio (SNR) values compared to single-pixel raster scan solutions due to the unfocused beam [1]. Additionally, the scanned areas become less scalable because their size is limited by the size of the available arrays. Thus, large objects must still be scanned in parts that can later be combined using special stitching techniques [33, 34]. However, this requires additional time and computing resources.

Another approach is single-pixel imaging with spatial filtering [35, 36], where the specifically designed static or dynamic optical filters are placed in sequence in the expanded beam after the sample to alter the intensity distribution. Such a beam is later focused on the single-pixel detector, and the image of the investigated sample is reconstructed numerically. Depending on beam modulators, such technique can provide images as large as 1200x1200 pixels in frequencies up to 13 THz [37]. However, producing high-quality modulation masks requires advanced manufacturing techniques, thereby significantly increasing equipment costs [35]. Therefore, due to their simplicity, versatility, cost-efficiency, and flexibility, raster scanning THz imaging systems remain an attractive, widespread, and universal solution, despite their slow data acquisition rate [2].

Major progress has occurred in the field of post-processing of THz images in the last decade [21]. During this time, methods have been developed to increase the spatial resolution of images [38, 39], reduce noise [15, 40], and deal with blur [18, 41]. Efforts have been made to eliminate interference fringes [19, 20] and model parameters of some other distortions [15, 29].

A special place in this regard belongs to methods based on convolutional neural networks (CNN), which, due to their high adaptability, make it possible to partially overcome the problem of initial conditions uncertainty. For instance, in [16], deep CNNs are used for noise modelling, whereas in [28, 40], they are used for THz image denoising. The authors of [38, 39] proposed CNN-based methods for improving THz image resolution, while the authors of [41] identified blurred THz images using CNN. In [42] the task of concealed object detection in THz images using an adapted YOLO network is considered. The method considers the low resolution of source images and contains a special block responsible for their denoising.

However, due to a lack of real-world image sets for preliminary analysis and training, the above-mentioned solutions rely primarily on empirical parameters and synthetic data, which makes them highly specialized. Moreover, there are tasks in THz image processing that have not yet received enough attention from researchers. The removal of compact impulse noise is one of them.

Scientists have considered the problem of eliminating impulse bursts from data for more than half a century, and during this time, many methods have been proposed [43, 44]. Most of them are based on order statistics [45] and represent some variations of the classic median filter [46, 47]. There are also solutions that are initially focused on severe cases with high impulse noise probabilities [48], but they still use masks and sorting to some extent. It should be noted that most methods for impulse noise removal are designed for uniformly distributed noise, which can be either random-valued or of salt-and-pepper type, whereas fewer solutions exist for

ISSN 1814-4225 (print)
ISSN 2663-2012 (online)

compact impulse noise elimination [26, 27].

The peculiarity of compact impulse noise is that, unlike uniformly distributed noise, its probability is not the same in different image areas, so along with severely affected areas, there may be areas where the noise is insignificant or absent [26, 27]. To eliminate compact impulse noise, one can use the same approaches as for ordinary impulse noise, but they should be adapted to account for the features of noise localization. Such adaptation may differ significantly from case to case, so the methods for eliminating compact impulse noise are also usually highly specialized.

Although compact impulse noise is a fairly common problem in raster-scanning THz imaging systems [24], the issue of its elimination has not yet been addressed in the literature. One possible reason for this is that impulse noise is usually considered a sign of poor data that is not worth fighting for, resulting from equipment errors. Sometimes this is true because compact impulse noise, even with a relatively small probability, can distort information details so much that it is impossible to preserve them during processing due to the small size of THz images [24]. Thus, it may seem that corrupted data should simply be dropped out or re-acquired. However, due to the laboriousness and time-consuming process of THz imaging, re-acquiring data is not always desirable. Therefore, identifying the conditions under which processing can give positive results is very important. Thus, this article, devoted to the study of improving the quality of terahertz images distorted by compact impulse noise, is expected to shed light on important practical aspects of THz visualization.

1.3. Objectives and tasks

The **goal** of this article is to investigate whether the quality of THz images containing compact impulse noise can be improved according to known visual quality metrics and to determine the conditions under which this can be achieved. To achieve the goal, within the framework of this publication, the following **tasks** must be solved:

1) to analyze impulse noise in a set of real-life THz images obtained by raster scanning systems and to evaluate its probabilities and localization features;

2) to create a generative model of compact impulse noise for simulation;

3) to investigate the relationship between the probability of impulse noise, image spatial resolution, filtering settings, and output image quality and provide recommendations;

4) to verify the recommendations based on real-life THz data.

The article is structured as follows: Section 2 contains the real and test image datasets used in the experiment, the description of the compact impulse noise model, and the research roadmap. Section 3 presents the filtering results obtained for both the test and real THz data and their analysis. Section 4 presents the discussion and provides prospects for further research. Section 5 concludes the article by summarizing the main points and results.

2. Materials and methods of research

The investigated THz images were obtained in the Center for Physical Sciences and Technology (Vilnius, Lithuania) using the direct imaging method at 0.253 THz with the setup shown in Fig. 1, a. Here, a field-effect transistor-based terahertz detector and emitter pair (Terahercinės technologijos, Vilnius, Lithuania) with linear polarization were used for radiation generation and registration. The beam from the emitter was collimated and then focused onto the sample using a pair of gold-coated off-axis parabolic (OAP) mirrors with a 50-mm diameter and a 100-mm focusing distance. The refocused beam was concentrated to the detector using another pair of OAP mirrors with a diameter of 50 mm. The sample was mounted on a motorized *xyz*-stage and raster scanned in the beam focus plane (*x*-*y*). In this experiment, the object was a metal frame with the vertically and horizontally oriented rectangular openings of different widths varying from 3 to 0.3 mm as shown in Fig. 1,b.

Fig. 2 shows several fragments of the frame with the biggest (3 mm) openings obtained at different distances from the OAP focusing on the sample that will be further referenced as Real1 (99 mm), Real2 (100 mm), Real3 (101 mm), and Real4 (105.5 mm). These are 8-bit images of size 153x156 pixels with the pixel size of 0.15 mm in both directions.

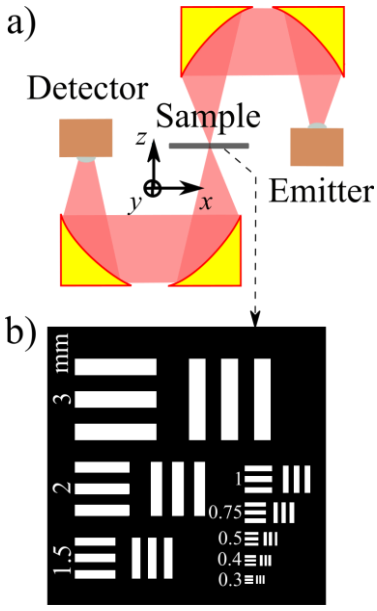

Fig. 1. The sample and the imaging setup

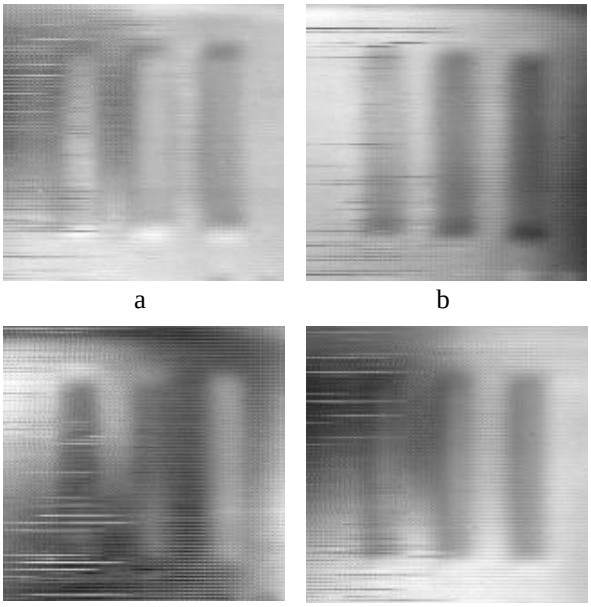

Fig. 2. THz images used in the experiment are as follows: Real1 (a), Real2 (b), Real 3 (c), Real4 (d)

These images are extensively blurred and contain interference amplitude variations that appear as darkened or highlighted areas. Parasitic (non-informative) texture in the form of alternating light and dark pixels and compact impulse noise that forms strips of light or dark shade are also present. This paper focuses on the latter, ignoring the other distortions.

The length of the strip-shaped impulse bursts is random but they are primarily localized in the left half of the image and have a horizontal orientation. The number of affected rows can range from 5-10% to about 50% of an image height in the most severe cases.

A functional describing the influence of impulse noise can be written as follows:

$$n_{imp}\left(k,l;f\left(k,l\right)\right)=\begin{cases}A_{imp}, & \text{with prob. } P_{imp}\\ f\left(k,l\right), & \text{with prob. } 1-P_{imp}\end{cases}, \quad (1)$$

where f(k,l) is the true (noise free) image (k = 1…K, l = 1…L, where K, L are the vertical and horizontal image dimensions in pixels, respectively); A_{imp} is the impulse noise amplitude that may be either constant or variable depending on the type of impulse noise; and P_{imp} is the probability of its occurrence.

In the case of compact impulse noise P_{imp} is not a constant but a complicated functional that depends on the pixel's location and the presence of bursts in the adjacent areas. Therefore, a few simplifications were made, and the strip-shaped noise was modeled as follows.

In the k-th row a string of A_{imp} values (constant in this case) that starts at a pixel $f(k,l_0)$ and is x pixels long may appear with the probability P_{imp}. To provide the noise localization in the left part of the image, l_0 is a whole random number in the range of 1 to L/4, while x is a whole random number in the range of 0 to $L-l_0$. It is important to emphasize that due to made simplifications, by the probability of the impulse noise, the probability of an image row being subject to the influence of noise, will be meant. Based on the observations from real-life THz data, the range of such probabilities will be 0.1 to 0.5.

Four test images were used: Test1 with the size 153x156 pixels, which is a complete match to the frame fragment with 3 mm wide openings, obtained at a spatial resolution 0.15x0.15 mm; Test2 with the size 77x78 pixels, which can be considered from two points of view: as an equivalent of the frame fragment with 1.5 mm wide openings or as an image of the same object as in Test1 but obtained at a spatial resolution 0.3x0.3 mm; Test 3 with the size 39x39 pixels, which models the frame fragment with 0.75 mm wide opening or a spatial resolution of 0.6x0.6 mm respectively; Test 4 with the size 20x20 pixels, which corresponds to 0.33 mm wide openings or a spatial resolution of 1.2x1.2 mm. Fig. 3 shows all test images, and Fig. 4 shows their versions distorted with compact impulse noise with different probabilities.

Because the filtering method should be simple and predictable, a classic median filter was selected [47]. Square sliding windows of sizes from 3x3 to 15x15 pixels, as well as rectangular windows with vertical spatial orientation, the dimensions of which varied from 1 to 5 in the horizontal direction and from 9 to 21 in the vertical direction, were considered.

The metrics PSNR and its modification PSNRHVSM [49] were used to quantitatively measure the filtering efficiency. Despite their common nature, using both of them in our task makes sense because they allow evaluation of filtering results from slightly different perspectives. Classic PSNR measures how closely the filtered image matches the original, whereas PSNRHVSM, which is better suited to human visual perception, assesses the visual appeal of the filtered images.

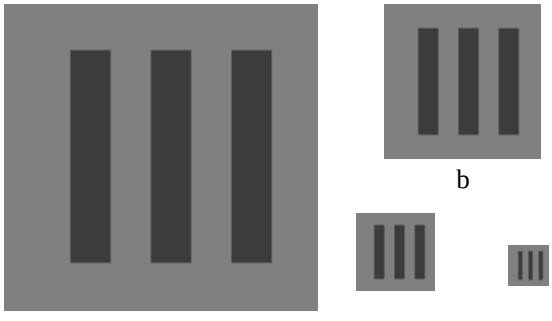

Fig. 3. Test images used in the experiment: Test1 (a), Test2 (b), Test3 (c), Test4 (d)

ISSN 1814-4225 (print)
ISSN 2663-2012 (online)

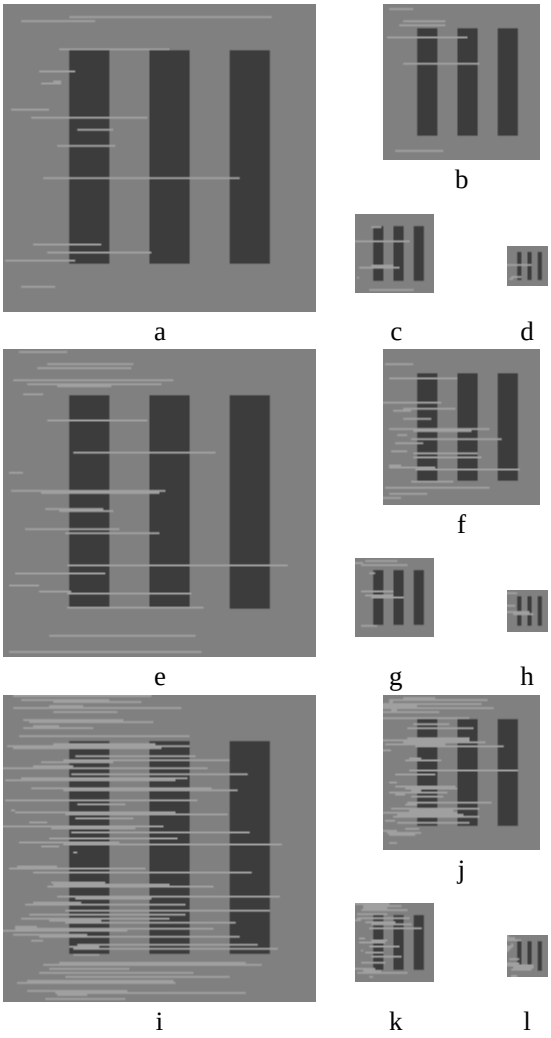

Fig. 4. Test images corrupted with compact impulse noise: P_{imp} = 0.1 (a – d), P_{imp} = 0.2 (e – h), P_{imp} = 0.5 (i – l)

Along with the values of PSNR and PSNRHVSM metrics, the difference values ΔPSNR and ΔPSNRHVSM have been analyzed. These values are calculated as:

$$\begin{aligned} \Delta\text{PSNR} &= \text{PSNR} - \text{PSNR}_{\text{init}}, \\ \Delta\text{PSNRHVSM} &= \text{PSNRHVSM} - \text{PSNRHVSM}_{\text{init}}, \end{aligned} \quad (2)$$

where $PSNR_{init}$ and $PSNRHVSM_{init}$ are obtained from the original noisy images, whereas PSNR and PSNRHVSM are obtained from the filtered images. Positive values of ΔPSNR and ΔPSNRHVSM mean that image quality has been improved by filtering, whereas negative values indicate that the quality after processing has worsened.

The research roadmap included the following steps:

1) analysis of compact impulse noise characteristics on real-life THz images;

2) modeling of compact impulse noise and creating an algorithm for its generation;

3) adding generated compact impulse noise to test images of different sizes;

4) processing test images with a median filter with different shapes and sizes of sliding windows and calculating filtering efficiency metrics;

5) formulating recommendations on the required sizes of source images and filtering settings;

6) verifying the given recommendations on real-life THz images.

3. Results Analysis

Since the problem of eliminating compact impulse noise in application to THz images has not yet been addressed in the literature, there are no specific methods to compare the results with. Therefore, this section will focus on the analysis of quantitative filtering quality criteria and the visual analysis of distorted and filtered test images. Additionally, due to the lack of specialized no-reference metrics adapted for working with THz images and their typical distortions, the results for real-life images will be analyzed based only on their visual inspection.

Fig. 5 shows the dependences of ΔPSNR and ΔPSNRHVSM on the sizes of square sliding windows of the median filter for different impulse noise probabilities. The values of $PSNR_{init}$ and $PSNRHVSM_{init}$ are given in Table 1.

The first observation that can be made from the presented data is that for the image Test4 processing in a square window even of the smallest size (3x3) leads to deterioration in image quality regardless of the impulse noise probability because of the distortions introduced by the filter. A similar situation is observed for the image Test3 with the only difference being that for P_{imp} = 0.1 a slight increase in PSNR and PSNRHVSM is spotted for a 3x3 window (0.73 and 0.94 dB, respectively). However, although the changes are visually noticeable (for PSNR and PSNRHVSM, the threshold for visual

Table 1

Initial values of PSNR and PSNRHVSM metrics for test images corrupted with compact impulse noise

Image	P_{imp}	$PSNR_{init}$, dB	$PSNRHVSM_{init}$, dB
Test1	0.1	29.14	26.88
	0.2	25.49	22.53
	0.5	19.34	16.27
Test2	0.1	29.14	26.4
	0.2	22.62	19.99
	0.5	20.02	16.15
Test3	0.1	24.76	21.43
	0.2	25.31	21.15
	0.5	19.93	16.37
Test4	0.1	25.5	23.49
	0.2	24.44	20.56
	0.5	21.29	17.34

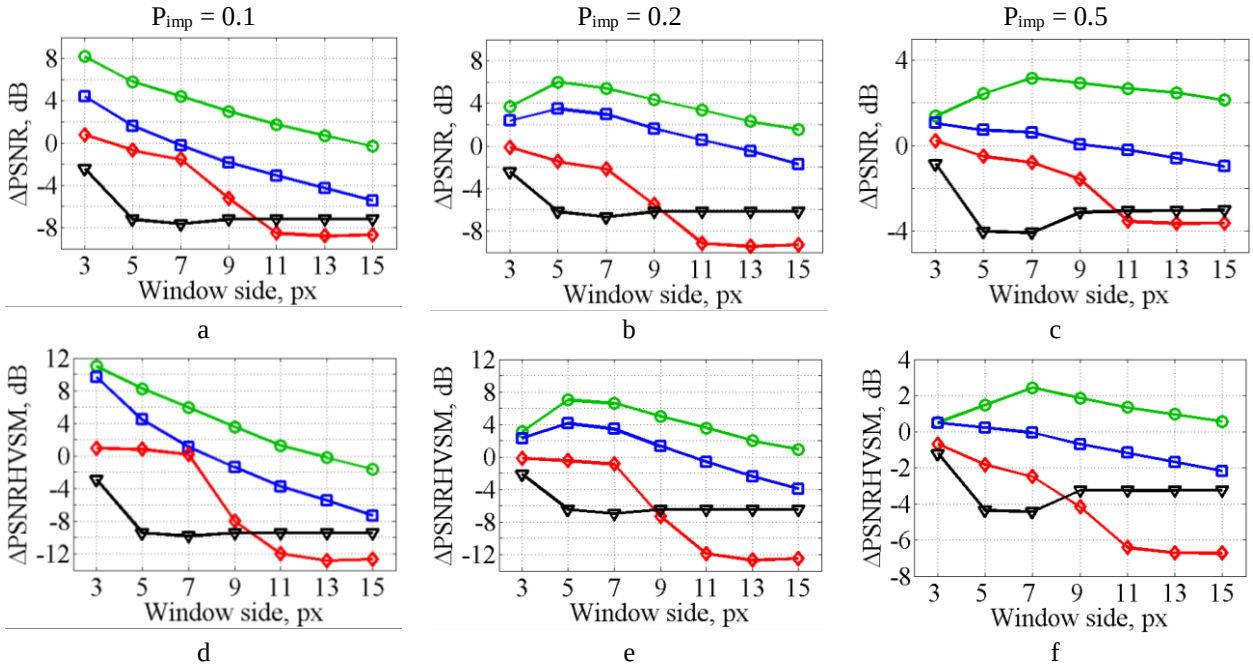

Fig. 5. Image quality improvement according to metrics PSNR(a – c) and PSNRHVSM (d – f) depending on the square window size for different impulse noise probabilities: P_{imp} = 0.1 (a, d), P_{imp} = 0.2 (b, e), P_{imp} = 0.5 (c, f); Test1; Test2; Test3; Test4.

noticeability is 0.5 dB [50]), the obtained filtering result can hardly be considered satisfactory given the initially low image quality (Table 1).

The situation is significantly better for the Test2 image. For a low impulse noise probability and the smallest window size, the quality improvement due to filtering can be up to 4 dB and 10 dB for PSNR and PSNRHVSM, respectively. However, these values rapidly decrease as the window size increases, and starting with a 9x9 window, filtering begins to degrade the quality rather than improve it. A similar situation is observed for P_{imp} = 0.2, but the maximum efficiency occurs at a 5x5 window, and the quality improvement is only 3 and 4 dB by PSNR and PSNRHVSM, respectively. Starting with an 11x11 window filtering becomes impractical. At P_{imp} = 0.5, any significant improvement in quality due to filtering is no longer possible. Formally, there is a gain of 0.48 dB by PSNRHVSM, but with the low initial image quality (Table 1), such improvement does not make any noticeable difference.

For probabilities 0.1 and 0.2, the situation with the Test1 image is very similar to that with Test2, but the gain in quality due to filtering is somewhat higher (11 and 7 dB, respectively, according to PSNRHVSM). However, for the probability of 0.5, several features are noteworthy. First, image quality improvement is observed for all the considered window sizes in this case. Second, the maximum filtering efficiency occurs for a 7x7 window, reaching almost 2.5 dB according to PSNRHVSM.

Fig. 6 shows the results for rectangular windows. The meanings of markers and line colors are the same as in Fig. 5, while line types correspond to different window sizes in the horizontal direction (HWS): solid – 1 px, dashed – 3 px, dashed-dotted – 5 px.

The first conclusion that can be drawn from the presented data is that increasing the sliding window size in the horizontal direction decreases filtering efficiency, and this difference becomes more pronounced for smaller test images. The best filtering results are obtained for narrow windows that are only 1 px wide. The second striking feature is that quality improvement is possible even for images of minimal size with a high probability of impulse noise.

As for the window size in the vertical direction, for noise probabilities 0.1 and 0.2, its increasing leads to deterioration in filtering efficiency too, with the highest quality metrics' values occurring at the 9x1 windows. For P_{imp} = 0.5, maximum filtering efficiency shifts to larger windows; however, the optimal window size differs for different test images and, presumably, significantly depends on noise localization. For ease of analysis, Table 2 summarizes the sizes of square and rectangular windows for which the maximum values of PSNR and PSNRHVSM were obtained.

We would like to highlight several interesting points in the data presented in Table 2. First, it is the significantly higher PSNR and PSNRHVSM values observed for the images processed in rectangular windows (see the lines marked with green). PSNRHVSM exceeds 45 dB in some cases, indicating that the post-processed image is visually indistinguishable from the original. The case with the Test3 image at the noise

ISSN 1814-4225 (print)
ISSN 2663-2012 (online)

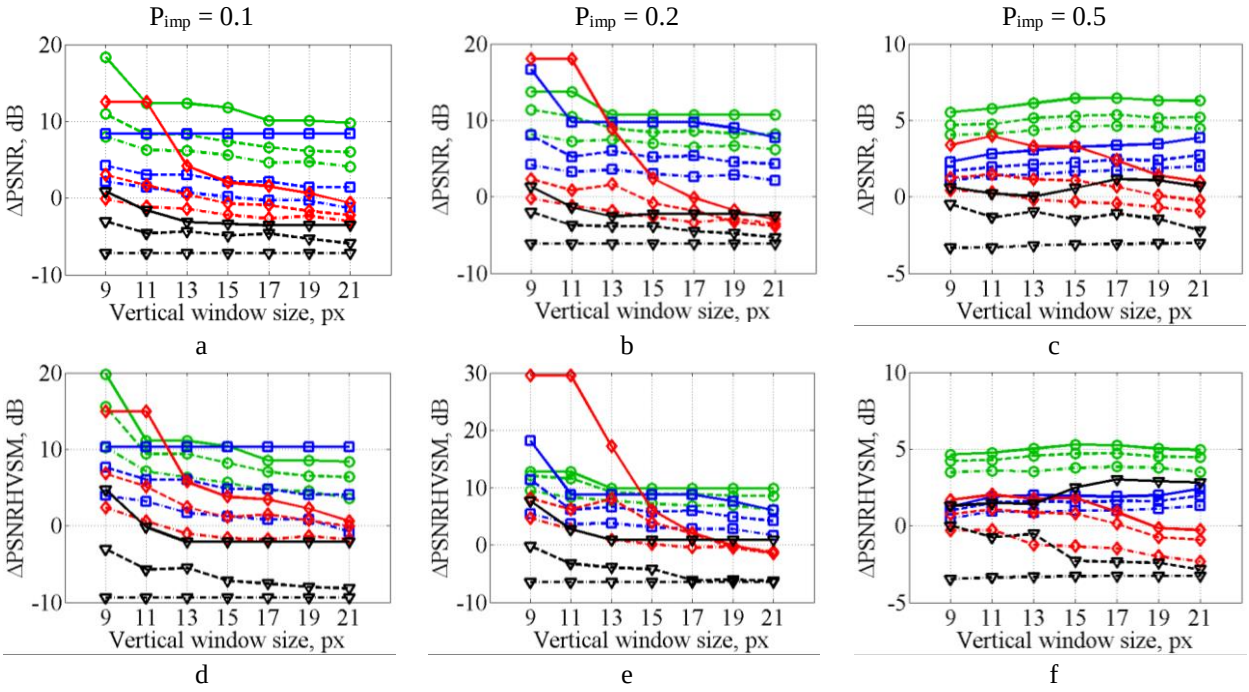

Fig. 6. Image quality improvement according to metrics PSNR(a – c) and PSNRHVSM (d – f) depending on the rectangular window size for different impulse noise probabilities: P_{imp} = 0.1 (a, d), P_{imp} = 0.2 (b, e), P_{imp} = 0.5 (c, f). Test1; Test2; Test3; Test4. HWS = 1 px; HWS = 3 px; HWS = 5 px.

probability of 0.2 is of particular interest in this regard. For median filter, 3x3 and 9x1 windows yield the same sample of 9 elements; however, in the former case, the processing results in a deterioration in image quality, while in the latter, the noise is perfectly eliminated. This can be explained as follows. For median filter, the breakaway point is 50%, which means that the filter will not return a normal value if the number of outliers is more than half of the sample size. Because the noise is localized in rows, even two such rows falling within the 3x3 window will result in six anomalous values, which is more than half of the sample. Simultaneously, for a 9x1 window, two noisy lines will yield only two anomalous values in the filter aperture, which is significantly less than 50%. If the noise probability is 0.2, the average number of noisy lines in a 9x1 filter window is 2, which explains its good performance. However, if the noise probability is approximately 0.5, a larger window size is better because it decreases the probability of exceeding the breakaway point.

The second interesting point concerns the Test4 image results. For rectangular windows, the ΔPSNR and ΔPSNRHVSM values differ significantly. While ΔPSNR values are about 1 dB, indicating that the processing result is only slightly closer to the original, the gain in PSRRHVSM ranges from 3 to 7.65 dB, demonstrating a significant improvement in visual quality. To understand the source of this difference and which metric to trust in this case, the images must be visually analyzed after processing.

The test images processed with median filter with the square and rectangular windows of sizes mentioned in Table 2 are presented in Figs. 7 and 8, respectively.

Even with fairly large images (Test1 and Test2) and low noise probabilities (0.1 and 0.2), the use of square windows results in incomplete noise elimination. Although objects are generally identified better compared to the ones in the noisy images (Fig. 4), their shapes can be significantly distorted, especially in smaller images. Consider the image in Fig. 7,d as an example. Although the noise probability is only 0.1, due to the specific localization of noise strips, filtering resulted in a significantly shortened first slit, while some parts in the middles of the first two slits were replaced with the background, so that the object's shape became unrecognizable. It is worth noting that in this case the values of ΔPSNR and ΔPSNRHVSM were negative, indicating the absence of quality improvement, but now there is visual proof why the filtering result cannot be considered acceptable.

At P_{imp} = 0.5, the situation is somewhat worse. Even for the Test1 image, a significant portion of the noise was not removed, while the object's shape was significantly affected, which is particularly noticeable at the slit edges and corners. For smaller images, identifying some of the slits is even more problematic, as they are still partly obscured by residual bands of compact impulse noise that, due to filtering, took the form of wider spots, rendering the image more unpleasant.

When rectangular windows are used, the processing

Table 2

Maximum values of PSNR and PSNRHVSM achieved after filtering and the corresponding window sizes

Image	P_{imp}	Window size, px	PSNR, dB	ΔPSNR, dB	PSNRHVSM, dB	ΔPSNRHVSM, dB
Test1	0.1	3x3	37.32	8.18	37.88	11
		9x1	**47.48**	18.34	**46.64**	19.76
	0.2	5x5	31.49	6	29.53	7
		9x1	39.24	13.75	35.27	12.74
	0.5	7x7	22.51	3.16	18.7	2.43
		15x1	25.80	6.45	21.56	5.29
Test2	0.1	3x3	33.53	4.39	36.06	9.65
		9x1	37.51	8.36	36.71	10.31
	0.2	5x5	26.09	3.47	24.12	4.12
		9x1	39.27	16.64	38.15	18.15
	0.5	3x3	21.08	1.06	16.62	0.48
		21x1	23.88	3.86	18.55	2.4
Test3	0.1	3x3	25.49	0.73	22.37	0.94
		9x1	37.28	12.52	36.39	14.96
	0.2	3x3	25.15	-0.17	20.96	-0.19
		9x1	**43.30**	17.99	**50.66**	29.5
	0.5	3x3	20.13	0.2	15.67	-0.7
		11x1	23.9	3.97	18.4	2.03
Test4	0.1	3x3	23.03	-2.47	20.61	-2.88
		9x1	26.36	0.86	28.21	4.72
	0.2	3x3	22.01	-2.43	18.43	-2.13
		9x1	25.74	1.3	28.21	7.65
	0.5	3x3	20.44	-0.85	16.12	-1.22
		17x1	22.44	1.15	20.36	3.01

results for the noise probabilities of 0.1 and 0.2 are quite good. In some cases, the filtered images are almost indistinguishable from the original, while others exhibit slight distortions at boundaries or corners, with little effect on the object's shape and size. The exception is the previously mentioned Test4 image. As shown in Figs. 8,d and 8,h, the noise has been eliminated completely, and the images appear more pleasing, as indicated by the high values of ΔPSNRHVSM. However, the dark rectangular gaps spread vertically, and this difference from the original causes the decrease in ΔPSNR values. Since the main purpose of THz visualization is to detect hidden objects or study their features, significant distortions of the object's size and shape are unacceptable, rendering this processing result unsatisfactory despite the improvement in visual quality according to quantitative criteria.

A similar situation is observed for P_{imp} = 0.5; however, the distortions have already been introduced here, while the noise has not been completely removed. Again, this effect becomes more pronounced as the size of the image under processing decreases. The localization of noise is also very important. If the outburst lines are dense, they might turn into wide spots that are even less visually pleasing than the original stripes after processing.

Considering the results in Fig. 8, i – l, only the filtered Test1 image can be seen as conditionally acceptable, as the shape and size of the object are not affected as significantly, whereas the object is more legible and the image in general appears more pleasing compared to its noisy version (see Fig. 4,i). However, if automatic algorithms are used to extract object parameters instead of expert visual assessment, such filtering-induced distortions may significantly reduce analysis accuracy.

Overall, the following preliminary conclusions can be drawn from the analysis of test images. With relatively low compact impulse noise probabilities (up to 0.2) and image sizes of at least 40x40 pixels, successful noise elimination is possible, improving image quality to approximately 40-45 dB, which means that the image after processing matches the original quite well. This requires a spatially adapted median filter with a vertically oriented rectangular sliding window. The recommended window size is 9x1. If the probability of impulse noise is higher (up to 0.5), the image quality can still be improved with the aforementioned filter, but the window size may need to be increased to 15x1. The window size for each case should be chosen based on the noise localization

ISSN 1814-4225 (print)
ISSN 2663-2012 (online)

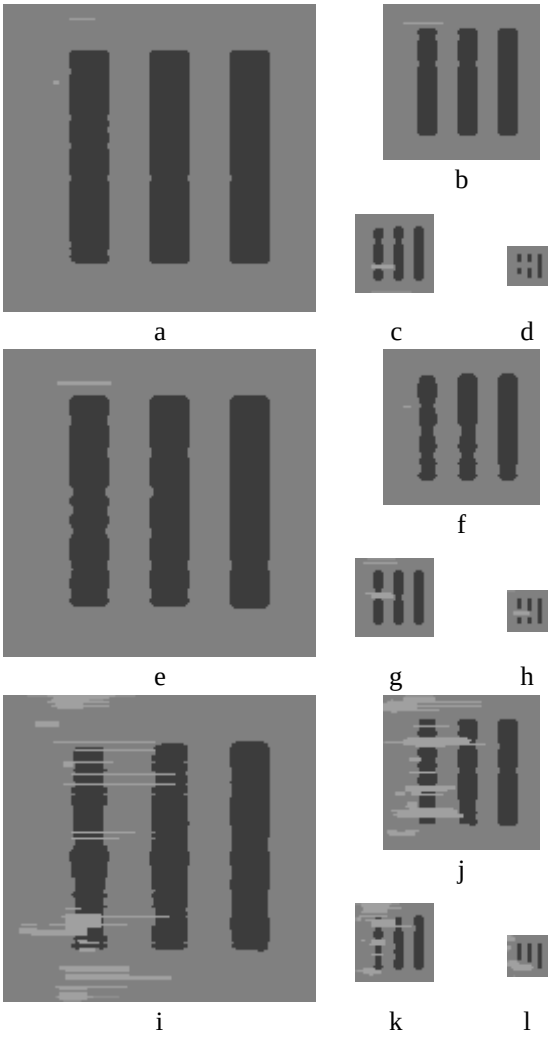

Fig. 7. Test images processed with median filter with square sliding windows: P_{imp} = 0.1 (a – d), window size is 3x3 (a – d); P_{imp} = 0.2 (e – h), window size is 5x5 (e, f) and 3x3 (g, h); P_{imp} = 0.5 (i – l), window size is 7x7 (i) and 3x3 (j – l)

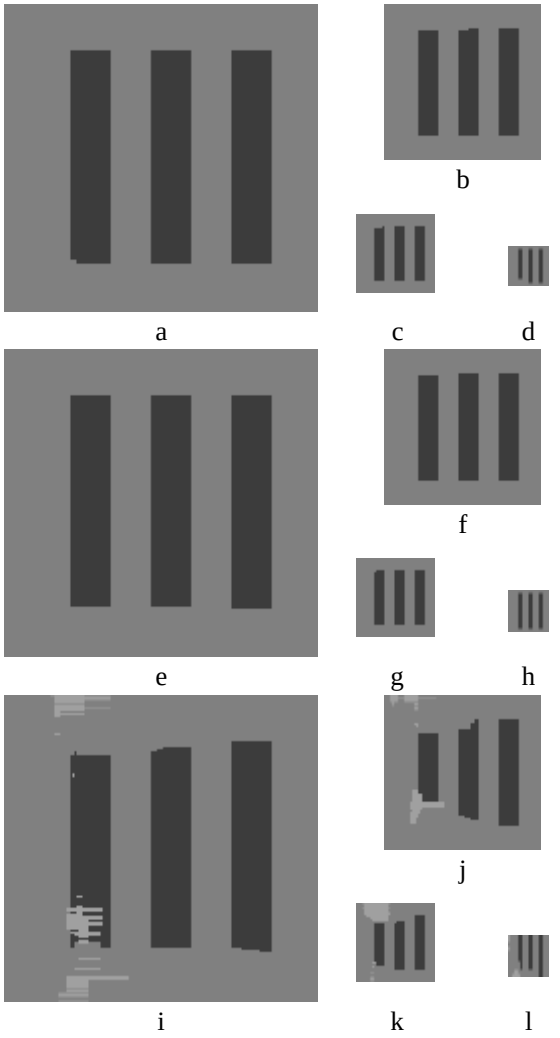

Fig. 8. Test images processed with median filter with rectangular sliding windows: P_{imp} = 0.1 (a – d), window size is 9x1 (a – d); P_{imp} = 0.2 (e – h), window size is 9x1 (e – h); P_{imp} = 0.5 (i – l), window size is 15x1 (i), 21x1 (j), 11x1 (k), and 17x1 (l)

(density) and the object being studied. In addition, to minimize introduced distortions, it is desirable that the image size is of at least 100x100 pixels.

We test these preliminary recommendations on real THz images. Fig. 9 shows the results for images Real1, Real2, Real3, and Real4 obtained using a median filter with square windows of 5x5 and 7x7 pixels, as well as rectangular windows of 9x1, 15x1, and 15x3 pixels.

The images processed in windows 5x5 and 7x7 appear noticeably under filtered. The residuals of impulse noise are well seen in some of their parts, while it was transformed into spots in the areas of its highest density. This is particularly noticeable in the left part of the Real1 image (Fig. 9,e) and in the lower part of the Real3 image (Fig. 9,g). Significant blurring and distortion of the edges are observed in some places (for example, in the upper left part of the Real4 image (Fig. 9,h)). Compared to 5x5 window, 7x7 window provides slightly better noise suppression, yet blurring of the edges is more pronounced.

Using 1 pixel wide rectangular windows yields interesting results. These windows allow to effectively remove strip-shaped compact impulse noise while preserving edges and texture. The 9x1 window (Fig. 9, m – p) is clearly insufficient for the existing noise probability, so traces of partially under removed impulse strips are visible in some places, whereas the 15x1 window performs quite well removing most of the noise manifestations (Fig. 9, q – t).

In this study, we specifically focused on impulse noise, ignoring other types of distortion. In this regard, the result for a 15x1 window with the compact impulse noise removed and the texture preserved is quite acceptable, although the texture is non-informative. If expert evaluation of the image is followed by filtering, this texture will not interfere with analysis because it does not hinder the evaluation of the object's shape and size. However, if texture removal is also required for

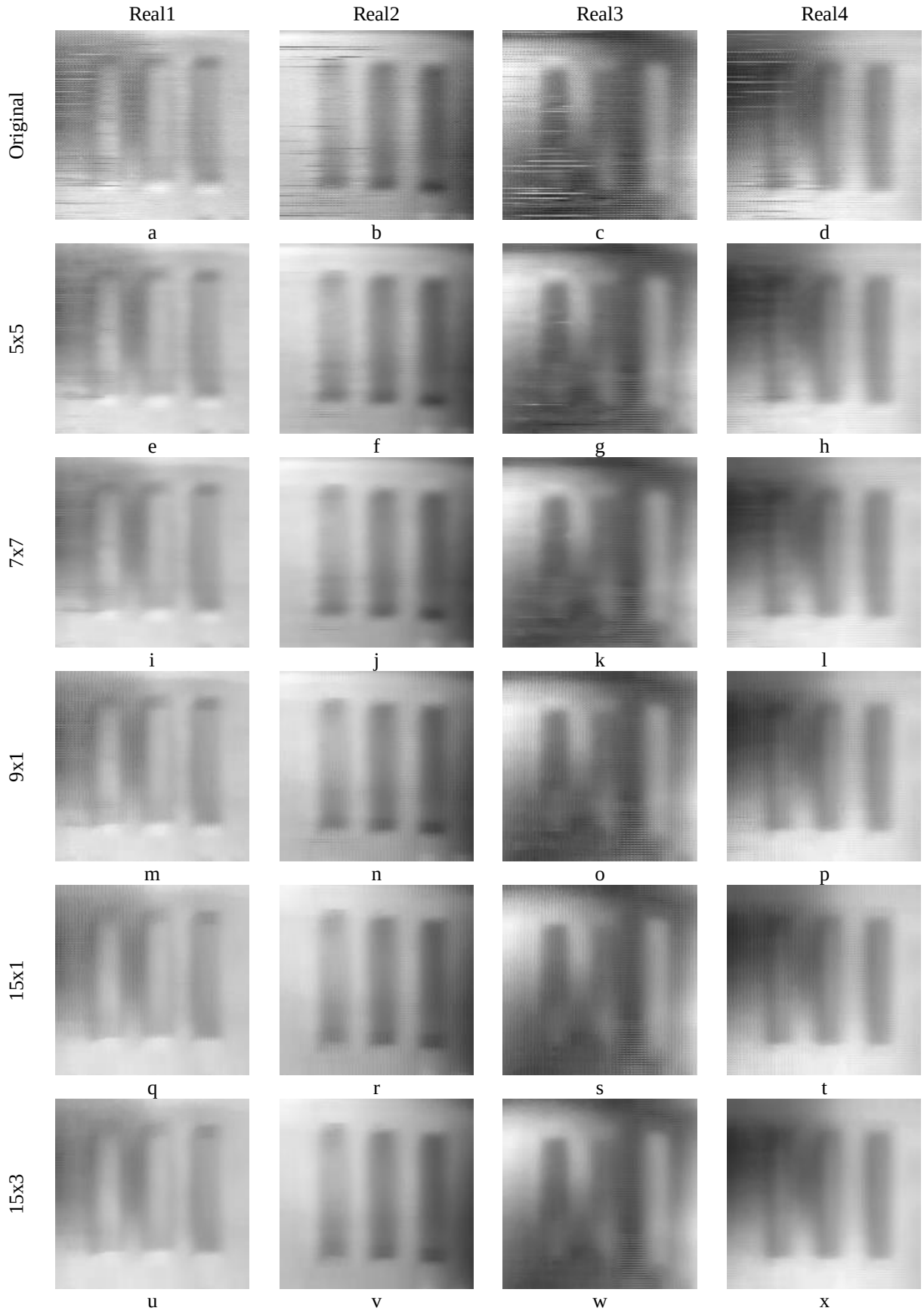

Fig. 9. THz images Real1 (a, e, i, m, q, u), Real2 (b, f, j, n, r, v), Real3 (c, g, k, o, s, w), and Real4 (d, h, l, p, t, x) original (a – d) and processed with median filter with windows of size 5x5 (e – h), 7x7 (i – l), 9x1 (m – p), 15x1 (q – t), and 15x3 (u – x)

ISSN 1814-4225 (print)
ISSN 2663-2012 (online)

subsequent processing (for example, to increase the accuracy of blind methods for object or edge recognition), this can be accomplished by increasing the window size to 15x3. The results for these sliding windows are shown in Fig. 9, u – x. The texture is successfully suppressed, while the edges are still clear. There are a few areas for the Real3 image (Fig. 9,w) where the texture was very intense and partly remained after filtering, but those areas can be additionally processed if required.

Overall, the results confirm the conclusions and recommendations drawn from the test images. If the impulse noise is localized in the form of stripes with a probability of occurrence no greater than 0.5, its successful removal with minimal distortion of the useful signal is viable. A spatially adaptive median filter is sufficient for this purpose, offering a robust and predictable solution that also features high performance. For horizontally oriented noise stripes, rectangular sliding windows with horizontal dimensions in the range of 1-3 pixels and vertical dimensions of 9-15 pixels. The processed image size should be at least 100x100 pixels.

The proposed approach can also be applied to vertically oriented compact impulse noise, but the sliding windows of the filter should be positioned horizontally (perpendicular to the raster scanning direction).

4. Discussion

The results presented in this paper are of great interest to the THz community, where the constant pursuit of simplicity, compactness, and affordability in imaging equipment places significant limitations on the quality of the source data. Using a simple and fast processing method considered in this work can help restore the information value of data that would otherwise have to be re-acquired, expending additional resources.

The requirements for the minimum image area containing the object of interest of 100x100 pixels described in this paper are quite feasible even for the simplest setups. However, several important points should be clarified.

In this case, the choice of test images and the shape of the objects in them were determined by the shape of the test plate traditionally used to study the performance of THz imaging systems. In real-world conditions, object shapes can be more complex and detailed, which may impose additional restrictions on both the required image size and the available options for filter windows. Therefore, one possible direction for future research could be to investigate the influence of object shape on potential filtering efficiency, followed by refinement of practical recommendations.

Another promising direction is the joint processing of multiple images. These could be conventional channels obtained by recording at close frequencies or images registered at different distances from the source but with identical standing wave phases.

Some positive results could be obtained by refining the compact impulse noise model and using other filters. The Abreu filter [48], designed to specifically address high-probability impulse noise, seems the most promising in this regard.

Finally, no-reference visual quality metrics could be very helpful in analyzing the efficiency of real-life data processing. Although specialized metrics for THz images do not yet exist, modern metrics designed with combined distortions in mind, such as [51], could be applied to these tasks. However, their adequacy in the presence of certain distortion combinations should be preliminarily tested, which is one more direction for future research.

Nevertheless, even at this stage, the results of this research highlight one important thing: given that the size of a source image is above the required minimum, even if the noise probability is quite high, the quality of such image can still be improved to the point sufficient for subsequent information extraction (either manually by an expert or by applying automatic tools). This significantly expands the scope of THz imaging tools' application, as it allows for partial compensation of equipment limitations.

5. Conclusions

The main contribution of this study is the confirmation of the possibility of improving the quality of terahertz images distorted by compact impulse noise at the post-processing stage and the formulation of practical recommendations on the parameters of processed images, the filtering methods used, and their settings that make such enhancement possible.

Terahertz images obtained using a single-detector direct imaging setup were analyzed, and the probabilities and localization features of impulse noise in them were studied. Noise takes on a strip-shaped compact form and is oriented along the raster scanning direction, while the probability of its occurrence typically ranges between 0.1 and 0.5.

Numerical simulation on a set of test images of different sizes has shown that using a spatially adapted median filter, such noise can be effectively eliminated. Its highest efficiency in terms of noise suppression and information detail preservation has been achieved with rectangular sliding windows that are 1 to 3 pixels wide and 9 to 15 pixels high. The sliding window size for each situation should be chosen considering the impulse noise probability and image size. Generally, it is desirable for the original image size to be at least 100x100 pixels and this size should be increased if an object has a

complicated shape or if there are important small information details. In some cases, the effective elimination of impulse noise might be possible for smaller images too (starting from 40x40 pixels), but for this, the noise probability should be relatively low (no higher than 0.2).

The proposed approach for eliminating compact impulse noise was tested on real-life terahertz images, and the formulated recommendations were confirmed to be adequate.

The enhancement of terahertz image quality is a complex process that involves multiple stages, and noise removal is only one of them. Since noise characteristics can vary significantly even across images of the same object obtained with the same setup, analyzing them and selecting appropriate noise-reduction methods must be done on a case-by-case basis. Thus, only by gathering information about possible noise variations in terahertz images can there be an aspiration to yield more universal solutions for their processing in the future.

Contributions of authors: conceptualization, methodology – **Viktoriia Abramova, Sergiy Abramov;** formulation of tasks, analysis – **Viktoriia Abramova, Sergiy Abramov, Ignas Grigelionis;** obtaining a dataset of THz images – **Ignas Grigelionis, Linas Minkevičius;** development of model, software, verification – **Viktoriia Abramova, Sergiy Abramov;** analysis of results, visualization – **Viktoriia Abramova;** writing, original draft preparation – **Viktoriia Abramova, Ignas Grigelionis**; review and editing – **Sergiy Abramov, Linas Minkevičius.**

Conflict of Interest

The authors declare that they have no conflict of interest in relation to this research, whether financial, personal, authorship or otherwise, that could affect the research and its results presented in this paper.

Financing

This study was partially funded by the Research Council of Lithuania (LMT) project number P-LU-PAR-25-23.

Data Availability

The manuscript has no associated data.

Use of Artificial Intelligence

The authors confirm that they did not use artificial intelligence technologies when creating the current work.

Acknowledgments

The authors are grateful to professors Volodymyr Lukin and Gintaras Valušis for fruitful discussions and useful insights during the process of preparation of this article.

All the authors have read and agreed to the published version of this manuscript.

References

1. Li, X., Li, J., Li, Y.,Ozcan, A., & Jarrahi, M. High-throughput terahertz imaging: progress and challenges. *Light: Science & Applications*, 2023, no. 12, article no. 233. DOI: 10.1038/s41377-023-01278-0.

2. Valušis, G., Lisauskas, A., Yuan, H., Knap, W., & Roskos, H. G. Roadmap of Terahertz Imaging 2021. *Sensors*, 2021, vol. 21, iss. 12, article no. 4092. DOI: 10.3390/s21124092.

3. Kaluza, M., Nieradka, A., Komorowski, P., & Siemion, A. Challenges and Limitations of Terahertz Phase Imaging Method. *Photonics Letters of Poland*, 2024, vol. 16, no. 4, pp. 82-86. DOI: 10.4302/plp.v16i4.1307.

4. Balzer, J., Saraceno, C., Koch, M., Kaurav, P., Pfeiffer, U., Withayachumnankul, W., Kürner, T., Stöhr, A., El-Absi, M., Abbas, A., Kaiser, T., & Czylwik, A. THz systems exploiting photonics and communications technologies. *IEEE Journal of Microwaves*, 2023, vol. 3, iss. 1, pp. 268-288. DOI: 10.1109/JMW.2022.3228118.

5. Tao, Y. H., Fitzgerald, A. J., & Wallace, V. P. Non-contact, non-destructive testing in various industrial sectors with terahertz technology. *Sensors*, 2020, vol. 20, iss. 3, article no. 712. DOI: 10.3390/s20030712 .

6. Karaliūnas, M., Nasser, K. E., Urbanowicz, A., Kašalynas, I., Bražinskenė, D., Asadauskas, S., & Valušis, G. Non-destructive inspection of food and technical oils by terahertz spectroscopy. *Scientific Reports*, 2018, vol. 8, article no. 18025. DOI: 10.1038/s41598-018-36151-3.

7. Takida, Y., Nawata, K., & Minamide, H. Security screening system based on terahertz-wave spectroscopic gas detection. *Optics Express*, 2021, vol. 29, iss. 2, pp. 2529-2537. DOI: 10.1364/OE.413201.

8. Yıldırım, İ. O. *Terahertz Stand-Off Imaging for Security Applications*. Ph.D. – Doctoral Program. Middle East Technical University, 2023. 151 p.

9. Cong, M., Li, W., Liu, Y., Bi, J., Wang, X., Yang, X., Zhang, Z., Zhang, X., Zhao, Y. N., Zhao, R., & Qiu, J. Biomedical application of terahertz imaging technology: a narrative review. *Quantitative Imaging in Medicine and Surgery*, 2023, vol. 13, iss. 12, pp. 8768-8786. DOI: 10.21037/qims-23-526.

10. Selvaraj, M., Sreeja, B. S., & Aly, M. Terahertz-based biosensors for biomedical applications: A review. *Methods*, 2025, vol. 234, pp. 54-66. DOI: 10.1016/j.ymeth.2024.12.001.

11. Krügener, K., Ornik, J., Schneider, L. M., Jackel, A., Koch-Dandolo, C. L., Castro-Camus, E.,

ISSN 1814-4225 (print)
ISSN 2663-2012 (online)

Riedl-Siedow, N., Koch, M., & Viol, W. Terahertz Inspection of Buildings and Architectural Art. *Applied Sciences*, 2020, vol. 10, iss. 15, article no. 5166. DOI: 0.3390/app10155166.

12. Reyes-Reyes, E. S., Carriles-Jaimes, R., D'Angelo, E., Nazir, S., Koch-Dandolo, C. L., Kuester, F., Jepsen, P. U., & Castro-Camus, E. Terahertz time-domain imaging for the examination of gilded wooden artifacts. *Scientific Reports*, 2024, vol. 14, iss. 1, article no. 6261. DOI: 10.1038/s41598-024-56913-6.

13. Artesani, A., Abate, F., Lamuraglia, R., Baldo, M. A., Menegazzo, F., & Traviglia, A. Integrated Imaging and Spectroscopic Analysis of Painted Fresco Surfaces Using Terahertz Time-Domain Technique, *Heritage*, 2023, vol. 6, iss. 7, pp. 5202-5212. DOI:10.3390/heritage6070276.

14. Cosentino, A. Terahertz and cultural heritage science: examination of art and archaeology. *Technologies*, 2016, vol. 4, iss. 1, article no. 6. DOI: 10.3390/technologies4010006.

15. Abramova, V., Abramov, S., Lukin, V., Grigelionis, I., Minkevičius, L., & Valušis, G. Improvement of terahertz images by adaptive discrete cosine transform (DCT)-based denoising. *Lithuanian Journal of Physics*, 2022, vol. 62, iss. 4, pp. 267-276. DOI: 10.3952/physics.v62i4.4823.

16. Sebastian, R. R., Guiramand, L., & Blanchard, F. Noise modelling using Deep CNN for Terahertz Super-Resolution Imaging. *2023 Photonics North (PN)*, Montreal, QC, Canada, 2023, pp. 1-2. DOI: 10.1109/PN58661.2023.10223028.

17. Abramova, V., Abramov, S., Lukin, V., Grigelionis, I., Minkevičius, L., Valušis, G. Investigation of blur kernel of terahertz images. *Lithuanian Journal of Physics*, 2023, vol. 63, no. 3, pp. 113-130. DOI: 10.3952/physics.2023.63.3.8.

18. Ljubenović, M., Zhuang, L., De Beenhouwer, J., & Sijbers, J. Joint deblurring and denoising of THz time-domain images. *IEEE Access*, 2020, vol. 9, pp. 162-176. DOI: 10.1109/ACCESS.2020.3045605.

19. Xu, L., Fan, W., & Liu, J. Suppression of the fluctuation effect in terahertz imaging using homomorphic filtering. *Chinese Optics Letters*, 2013, vol. 11, no. 8, article no. 081201. DOI: 10.3788/COL201311.081201.

20. Wang, Y., Chen, L., Chen, T., Xu, D., Shi, J., Ren, Y., Li, C., Zhang, C., Liu, H., & Wu, L. Interference elimination in terahertz imaging based on inverse image processing, *Journal of Physics D: Applied Physics*, 2018, vol. 51, no. 32, article no. 5101, DOI: 10.1088/1361-6463/aad0ca.

21. Kundu, B. K., & Pragti. THz Image Processing and Its Applications, in: *Generation, Detection and Processing of Terahertz Signals*. *Lecture Notes in Electrical Engineering*, vol. 794, Springer, Singapore, 2022, pp. 123–137. DOI: 0.1007/978-981-16-4947-9_9.

22. Jokubauskis, D., Minkevičius, L., Seliuta, D., Kašalynas, I., & Valušis, G. Terahertz homodyne spectroscopic imaging of concealed low-absorbing objects, *Optical Engineering*, 2019, vol. 58, iss. 2, article no. 023104. DOI: 10.1117/1.OE.58.2.023104.

23. Lou, X., Hou, L., Guo, G., & Shi, W. Restoration of terahertz continuous wave image obtained by continuous scan mode with large time constant. *Applied Optics*, 2014, vol. 53, iss. 32, article no. 7735–40. DOI: 10.1364/ao.53.007735.

24. Abramova, V., Abramov, S., Lukin, V., Grigelionis, I., Minkevičius, L., Valušis, G. Problems of terahertz images quality enhancement, *Advanced Properties and Processes in Optoelectronic Materials and Systems (Apropos 19)*, Vilnius, Lithuania, 2024, article no. S8-O3. Available at: https://apropos.ftmc.lt/wp-content/abstracts19/files/S8-O3-Viktoriia-Abramova-Problems-of-terahertz-images-quality-enhancement-06fqn.pdf (accessed 14.10.2025).

25. Ibrahim, H., Neo, K. C., Teoh, S. H., Theam Foo Ng, T. F., Chieh, D. C. J., & Hassan, N. F. Impulse Noise Model and Its Variations, *International Journal of Computer and Electrical Engineering*, 2012, vol. 4, no. 5, pp. 647-650. DOI: 10.7763/IJCEE.2012.V4.575.

26. Tsymbal, O. V., Lukin, V. V., Koivisto, P. T., & Melnik, V. P. Removal of impulse bursts in satellite images, *Second IEEE International Workshop on Intelligent Data Acquisition and Advanced Computing Systems: Technology and Applications*, Lviv, Ukraine, 2003, pp. 324-329, DOI: 10.1109/IDAACS.2003.1249575.

27. Koivisto, P., Astola, J., Lukin, V., Melnik, V., Tsymbal, O. Removing Impulse Bursts from Images by Training-Based Filtering. *EURASIP Journal on Advances in Signal Processing*, 2003, article no. 472580. DOI: 10.1155/S1110865703211045.

28. Jung, S.-H., Yeo, W.-H., Maeng, I., Ji, Y., Oh, S. J., & Ryu, H.-C. Self-supervised deep-learning for efficient denoising of terahertz images measured with THz-TDS system, *Expert Systems with Applications*, 2025, vol. 271, article no. 126595. DOI: 10.1016/j.eswa.2025.126595.

29. Ahi, K. Mathematical modeling of THz point spread function and simulation of THz imaging systems. *IEEE Transactions on Terahertz Science and Technology*, 2017, vol. 7, pp. 747-754. DOI: 10.1109/TTHZ.2017.2750690.

30. Wu, Q., Hewitt, T. D. & Zhang, X. C. Two-dimensional electro-optic imaging of THz beams. *Applied Physics Letters*, 1996, vol. 69, pp. 1026-1028. DOI: 10.1063/1.116920.

31. Spickermann, G., Friederich, F., Roskos, H. G., & Bolivar, P. H. High signal-to-noise-ratio electro-optical terahertz imaging system based on an demodulating detector array. *Optics Letters*, 2009, vol. 34, pp. 3424-3426. DOI: 10.1364/OL.34.003424.

32. Li, X., Mengu, D., Yardimci, N. T., Turan, D., Charkhesht, A., Ozcan A., & Jarrahi, M. Plasmonic photoconductive terahertz focal-plane array with pixel super-resolution. *Nature Photonics*, 2024, vol. 18, pp. 139-148. DOI: 10.1038/s41566-023-01346-2.

33. Liu, P., Han, J., Tian, F., Wu, Z., & Wang, J. Research on image stitching technology for focal plane array terahertz imaging. *Proc. SPIE 10843, 9th International Symposium on Advanced Optical Manufacturing and Testing Technologies: Optoelectronic Materials and Devices for Sensing and Imaging*, 2019, article no. 108430Z. DOI: 10.1117/12.2506362.

34. Wu, X., Bai, F., Li, L., Gao, Y., Wang, W., & Cai, H. Unsupervised disparity-tolerant algorithm for terahertz image stitching. *Scientific Reports*, 2025, vol. 15, article no. 31159. DOI: 10.1038/s41598-025-16594-1.

35. Stantchev, R. I., Sun, B., Hornett, S. M., Hobson, P. A., Gibson, G. M., Padgett, M. J., & Hendry, E. Noninvasive, near-field terahertz imaging of hidden objects using a single-pixel detector. *Science Advances*, 2016, vol. 2, article no. e1600190. DOI:10.1126/sciadv.1600190.

36. Stantchev, R. I., Yu, X., Blu, T., & Pickwell-MacPherson, E. Real-time terahertz imaging with a single-pixel detector. *Nature Communications*, 2020, vol. 11, article no. 2535. DOI: 10.1038/s41467-020-16370-x.

37. Vallés, A., He, J., Ohno, S., Omatsu, T., & Miyamoto, K. Broadband high-resolution terahertz single-pixel imaging, *Optics Express*, 2020, vol. 28, article no. 28868-81. DOI:10.1364/oe.404143.

38. Long, Z., Wang, T., You, C., Yang, Z., Wang, K., & Liu, J. Terahertz image super-resolution based on a deep convolutional neural network, *Applied Optics*, 2019, vol. 58, iss. 10, pp. 2731-2735. DOI: 10.1364/AO.58.002731.

39. Li, Y., Hu, W., Zhang, X., Xu, Z., Ni, J., & Ligthart, L. P. Adaptive terahertz image super-resolution with adjustable convolutional neural network, *Optics Express*, 2020, vol. 28, iss. 15, pp. 22200-22217. DOI: 10.1364/OE.394943.

40. Dutta, B., Root, K., Ullmann, I., Wagner, F., Mayr, M., Seuret, M., Thies, M., Stromer, D., Christlein, V., Schür, J., Maier, A., Huang, Y. Deep learning for terahertz image denoising in nondestructive historical document analysis. *Scientific Reports*, 2022, vol. 12, article no. 22554. DOI: 10.1038/s41598-022-26957-7.

41. Chen, Z., Wang, C., Feng, J., Zou, Z., Jiang, F., Liu, H., & Jie, Y. Identification of blurred terahertz images by improved cross-layer convolutional neural network, *Optics Express*, 2023, vol. 31, iss. 10, pp. 16035-16053. DOI: 10.1364/OE.487324.

42. Cheng, A., Wu, S., Liu, X., Lu, H. Enhancing concealed object detection in active THz security images with adaptation-YOLO. *Scientific Reports*, 2025, vol. 15, article no. 2735. DOI: 10.1038/s41598-024-81054-1.

43. Judith.M.C, G., & Kumarasabapathy, N. Study and Analysis of Impulse Noise Reduction Filters. *Signal & Image Processing : An International Journal*, 2011, vol. 2, iss. 1, pp. 82-92. DOI: 10.5121/sipij.2011.2107.

44. Sen, A. P., Pradhan, T., Rout, N. K., & Kumar, A. Comparison of algorithms for the removal of impulsive noise from an image, *e-Prime – Advances in Electrical Engineering, Electronics and Energy*, 2023, vol. 3, article no. 100110. DOI: 10.1016/j.prime.2023.100110.

45. Liu, Y., & Lei, Z. Review of Advances in Active Impulsive Noise Control with Focus on Adaptive Algorithms. *Applied Science*, 2024, vol. 14, article no. 1218. DOI: 10.3390/app14031218.

46. Tukey, J. W., Cromwell, L. *Exploratory Data Analysis*. Pearson, 1977. 712 p.

47. Pitas, I., & Venetsanopoulos, A. N. Median Filters. In: *Nonlinear Digital Filters. The Springer International Series in Engineering and Computer Science*, 1990, vol. 84. Springer, Boston, MA. DOI: 10.1007/978-1-4757-6017-0_4.

48. Abreu, E., Lightstone, M., Mitra, S. K., & Arakawa, K. A new efficient approach for the removal of impulse noise from highly corrupted images, *IEEE Transactions on Image Processing*, 1996, vol. 5, no. 6, pp. 1012-1025. DOI: 10.1109/83.503916.

49. Ponomarenko, N., Silvestri, F., Egiazarian, K., Carli, M., Astola, J., Lukin, V. On between-coefficient contrast masking of DCT basis functions, *CD-ROM Proceedings of the Third International Workshop on Video Processing and Quality Metrics for Consumer Electronics*, Scottsdale, Arizona, USA, 2007, article no. VPQM-07. Available at: https://ponomarenko.info/vpqm07_p.pdf (accessed 14.10.2025).

50. Li, F., Krivenko, S., & Lukin, V. A Two-step Approach to Providing a Desired Visual Quality in Image Lossy Compression, *IEEE 15th International Conference on Advanced Trends in Radioelectronics, Telecommunications and Computer Engineering (TCSET)*, Lviv-Slavske, Ukraine, 2020, pp. 502-506. DOI: 10.1109/TCSET49122.2020.235483.

51. Oszust, M. No-reference quality assessment of noisy images with local features and visual saliency models. Information Sciences, 2019, vol. 482, pp. 334-349. DOI: 10.1016/j.ins.2019.01.034.

Received 14.10.2025, Received in revised form 21.12.2025
Accepted date 15.01.2026, Published date 22.01.2026

ПОКРАЩЕННЯ ТЕРАГЕРЦОВИХ ЗОБРАЖЕНЬ, ПОШКОДЖЕНИХ КОМПАКТНИМ ІМПУЛЬСНИМ ШУМОМ: ДОЦІЛЬНІСТЬ ТА ПРАКТИЧНІ РЕКОМЕНДАЦІЇ

В. В. Абрамова, С. К. Абрамов, Л. Мінкевічюс, І. Грігеліоніс

Предметом дослідження є процеси покращення терагерцових зображень низької якості завдяки цифровій обробці. **Метою** дослідження є вивчення можливості покращення візуальної якості терагерцових зображень, пошкоджених компактним імпульсним шумом, за збереження їхньої інформаційної цінності. **Завдання**,

ISSN 1814-4225 (print)
ISSN 2663-2012 (online)

що потребують вирішення: 1) проаналізувати імпульсний шум на реальних терагерцових зображеннях, отриманих растровими скануючими системами, та оцінити типовий діапазон його ймовірностей та особливості локалізації; 2) створити адекватну модель для генерування компактного імпульсного шуму; 3) встановити зв'язок між ймовірністю імпульсного шуму, роздільною здатністю зображення, налаштуваннями фільтрації та якістю вихідних зображень й надати відповідні рекомендації; 4) перевірити отримані результати на реальних терагерцових даних. **Методи** досліджень: математичне моделювання, числове моделювання, статистичний аналіз. Були отримані наступні **результати.** 1) Було визначено форму та характеристики локалізації компактного імпульсного шуму на терагерцових зображеннях, отриманих з допомогою однодетекторної установки прямої візуалізації та реалізовано відповідну генеративну статистичну модель. 2) З допомогою числового моделювання на наборі тестових зображень було досліджено можливість придушення цього шуму з використанням класичного медіанного фільтра та його модифікації з просторовою адаптацією. 3) Показано, що для зображень розміром не менше 100×100 пікселів та ймовірності імпульсного шуму до 0,5, фільтрація у вертикально орієнтованих прямокутних вікнах (від 9×1 до 15×1 пікселів) дає змогу покращити якість до 45 дБ згідно з метриками PSNR та PSNRHVSM, забезпечуючи ефективне придушення шуму зі збереженням деталей об'єкта. 4) Адекватність цих рекомендацій було підтверджено верифікацією на реальних терагерцових даних та підтверджено працездатність запропонованого підходу за наявності інших спотворень. **Висновки.** Наукова новизна отриманих результатів полягає у підтвердженні можливості надійного відновлення терагерцових зображень, сильно спотворених компактним імпульсним шумом, без їх повторного отримання, а також надання практичних рекомендацій щодо налаштувань фільтрації та вимог до вхідних терагерцових даних.

Ключові слова: обробка зображень, підвищення якості, терагерцові зображення, компактний імпульсний шум, растрові системи сканування.

Абрамова Вікторія Валеріївна – канд. техн. наук, доц. каф. інформаційно-комунікаційних технологій, Національний аерокосмічний університет «Харківський авіаційний інститут», Харків, Україна; науковий співробітник відділу оптоелектроніки, Центр фізики та технологій, Вільнюс, Литва.

Абрамов Сергій Клавдійович – канд. техн. наук, доц., доц. каф. інформаційно-комунікаційних технологій, Національний аерокосмічний університет «Харківський авіаційний інститут», Харків, Україна; старший інженер відділу функціональних матеріалів та електроніки, Центр фізики та технологій, Вільнюс, Литва.

Мінкевічюс Лінас – д-р філос., головний науковий співробітник, зав. відділу оптоелектроніки, Центр фізики та технологій, Вільнюс, Литва.

Грігеліоніс Ігнас – д-р філос., старш. наук. співроб. відділу оптоелектроніки, Центр фізики та технологій, Вільнюс, Литва.

Viktoriia Abramova – Candidate of Technical Sciences, Associate Professor at the Department of Information-Communication Technologies, National Aerospace University, Kharkiv, Ukraine; Researcher at the Department of Optoelectronics, Center for Physical Sciences and Technology, Vilnius, Lithuania,
e-mail: v.abramova@khai.edu, ORCID: 0000-0001-5802-5858, Scopus Author ID: 55225531900.

Sergiy Abramov – Candidate of Technical Sciences, Associate Professor at the Department of Information-Communication Technologies, National Aerospace University, Kharkiv, Ukraine; Senior Engineer at the Department of Functional Materials and Electronics, Center for Physical Sciences and Technology, Vilnius, Lithuania,
e-mail: s.abramov@khai.edu, ORCID: 0000-0002-8295-9439, Scopus Author ID: 7005979784.

Linas Minkevičius – PhD, Chief Researcher, Head of the Department of Optoelectronics, Center for Physical Sciences and Technology, Vilnius, Lithuania,
e-mail: linas.minkevicius@ftmc.lt, ORCID: 0000-0002-3831-8976, Scopus Author ID: 36667073000.

Ignas Grigelionis – PhD, Senior Researcher at the Department of Optoelectronics, Center for Physical Sciences and Technology, Vilnius, Lithuania,
e-mail: ignas.grigelionis@ftmc.lt, ORCID: 0000-0001-8383-3427, Scopus Author ID: 57225735461.